Low Index-Contrast Photonic Crystal Nanobeam Resonator Based on PMMA on Silica Substrate

A. I. Garifullin[a,b]*, V. K. Boldysheva [b], O. A. Ermishev [b], N. M. Arslanov[b,]**

[a] *Institute of Physics, Kazan Federal University, Kazan, Russia*

[b] *Kazan Quantum Center, Kazan National Research Technical University n.a. A.N. Tupolev – KAI, Kazan, Russia*

**e-mail: adel-garifullin@mail.ru*

***e-mail: narkis@yandex.ru*

Received November 10, 2025; revised November 15, 2025; accepted November 15, 2025

Abstract. The integrated photonics has been revolutionized by the development of photonic crystal cavities, which are essential for confining and controlling light at the wavelength scale. These structures are characterized by their ability to localize optical fields within a small mode volume V, and sustain them with a high-quality factor Q, a measure of optical energy storage. The Q/V ratio is a critical figure of merit, as it governs the strength of light-matter interactions, making such cavities indispensable for a wide range of applications. At the same time, polymers are a highly versatile class of materials for micro and nanofabrication. They have been actively used in photonics as they can be integrated and doped with a wide range of materials, providing structures with tunable photonic response. Thus, in this work the design of a one-dimensional polymeric photonic crystal resonator based on polymethyl-methacrylate and suspended in air, and placed on a silica substrate, is presented. Using the three-dimensional finite-difference time-domain method and deterministic high-Q design method, the polymeric photonic crystal cavity design and optimization are investigated theoretically. A high Q-factor of $5 \cdot 10^5$, small mode volume V of $0.81(\lambda/n_{cavity})^3$, and Purcell factor F of $4.7 \cdot 10^4$ for the suspended photonic crystal cavity at the resonant telecommunications wavelength of $\lambda = 1.55$ μm can be achieved. For the structure placed on a silica substrate a maximum Q-factor is $3 \cdot 10^2$, mode volume V is $0.88(\lambda/n_{cavity})^3$, and Purcell factor F is 26 at $\lambda \sim 1.55$ μm.

Keywords: photonic crystal nanobeam cavity, PMMA, silica, quality factor, mode volume, Purcell factor

1. INTRODUCTION

Polymeric materials are perspective in the fabrication of micro- to nano-scale devices. Examples of successful applications can be found in waveguides, large screen and flexible displays, solar cells, biomedical sensors [1]. The realization of all-polymer devices has proved challenging in the development of high-quality (Q) factor and small mode volume (V) optical resonators. Such optical

elements provide powerful means for enhancing the light-matter interaction, and have many exciting quantum optical applications including nonlinear optics, optomechanics, optical trapping, *etc*. [2]. The main types of optical resonators include whispering gallery mode cavities, Fabry-Perot cavities and photonic crystal (PhC) cavities [3-5].

Since the first publications of PhC structures [6, 7], PhC cavities have been actively used for observation and research quantum electrodynamical effects, such as coherent control of spontaneous emission, quantum interference, photon-atom bound state, modification of Lamb shift, modification of the electron electromagnetic mass, and others [8-10]. PhC resonators [11, 12] have demonstrated numerous advantages over other cavity geometries due to their wavelength-scale mode volumes and over-million *Q*-factors [2]. However, creation the polymeric high-*Q* PhC cavities is challenging due to the low index contrast between polymeric materials and substrate.

Quan Q. *et al.* [1] presented the design, fabrication and characterization of high-*Q* ($Q_{simulation}$ = $8.6 \cdot 10^4$ and $Q_{experiment}$ = $3.6 \cdot 10^4$ at telecommunication wavelength range, 1.50-1.55 μm) polymeric one-dimensional (1D) PhC nanobeam cavity made of ZEP520 resist (n_{cavity} = 1.54) on a CYTOP substrate ($n_{background}$ = 1.34) and clad with water/D_2O, creating an ultra-low index contrast of 1.15 and observed thermo-optical bistability at hundred-microwatt power level. A ridge waveguide perforated with elliptical air holes, the lattice period a = 550 nm.

Clevenson H. *et al*. [13] presented high-sensitivity, multi-use optical gas sensors based on a 1D PhC cavity. This suspended structure was made from polymethyl-methacrylate (PMMA) – a flexible polymer with $n_{cavity} \sim 1.52$ with periodic rectangular holes. A simulated *Q*-factor of $>1.07 \cdot 10^5$ was achieved. Experimentally, a *Q*-factor exceeding 10^4 was measured at λ = 627 nm, and an ultra-small mode volume *V* of $1.36(\lambda/n)^3$, where *n* is the refractive index of the polymer.

Gan X. *et al*. [14] introduced a 1D polymeric cavity-based optical sensor for measuring strain, displacement, and force that sets new records for similarly sized devices. Also, the structure was suspended in air and was made from PMMA 1D photonic crystal ladder cavity with a refractive index n_{cavity} =1.5 and a central defect created by a parabolic variation in the lattice constants with periodic rectangular holes. Lattice constant, *a*, was designed for operation in the visible range (fabricated with a between 265 nm and 285 nm). A maximum simulated *Q*-factor of $1.07 \cdot 10^5$ was predicted for the optimized design at a normalized wavelength a/λ=0.447. The measured nanocavities exhibited *Q*-factors exceeding $1.2 \cdot 10^4$, with some characterized as higher than 10^4. In a water environment with $n_{background}$ = 1.33, a moderately high *Q*-factor of $2.1 \cdot 10^3$ was simulated. The simulated mode volume *V* was $1.36(\lambda/n)^3$ for a polymeric resonator. Note that experimentally demonstrated resonant wavelength was in the visible range between 550 nm and 610 nm (568.1 nm, 606.1 nm).

Recently, Li X. *et al.* [15] theoretically and experimentally demonstrated a novel nanocavity-based polymer-on-insulator electro-optic modulator. It consisted of a polymeric PhC nanobeam cavity with ultra-low index-contrast ($n_{cavity}/n_{background}$ = 1.17) with periodic elliptical holes, where n_{cavity} = 1.699 (SEO100 C polymer) and $n_{background}$ = 1.45 (silica). This structure had a high *Q*-factor of $3.4 \cdot 10^4$ and small mode volume *V* of 22.8 $(\lambda/n_{cavity})^3$ at ~ 1.557 μm.

In this work, we present the design of a polymeric 1D PhC nanobeam resonator based on PMMA (n_{cavity} = 1.5) and suspended in air ($n_{background}$ = 1), and placed on a silica substrate ($n_{background}$ = 1.45). Based on three-dimensional (3D) finite-difference time-domain (FDTD) method (Ansys Lumerical FDTD Solutions, MEEP software package) and finite element method FEM (Comsol Multiphysics),

the 1D PhC nanobeam cavity design and optimization are investigated theoretically. A high Q-factor of $5 \cdot 10^5$, small mode volume V of $0.81(\lambda/n_{cavity})^3$, and Purcell factor F of $4.7 \cdot 10^4$ for low index-contrast $n_{cavity}/n_{background} = 1.5$ at the cavity resonant telecommunications wavelength $\lambda = 1.55$ μm can be achieved. For the extraordinary low index-contrast $n_{cavity}/n_{background} = 1.03$ a maximum Q-factor is $3 \cdot 10^2$, mode volume V is $0.88(\lambda/n_{cavity})^3$, and Purcell factor F is 26 at $\lambda = 1.55$ μm.

2. PHOTONIC CRYSTAL NANOBEAM CAVITY DESIGN

The 1D PhC nanobeam cavity design consists of a waveguide with periodic elliptical holes (Fig. 1a). We considered a cavity based on PMMA with refractive index $n_{cavity} = 1.5$ surrounded by air $n_{background} = 1$ (suspended PhC nanobeam cavity, Fig. 1b [16]). Note that fabrication of a suspended polymeric waveguide is challenging due to the flexible mechanical properties of polymers. For this purpose, in practice, a structure placed on a substrate is often used, and this substrate must be mechanically strong, with low refractive index and commercially available. One of the common materials of substrates is silica with $n_{background} = 1.45$ (Fig. 1c). The width of the proposed polymeric structure is $w_{nanobeam} = 3$μm, the thickness of the waveguide is $h_{nanobeam} = 1$ μm.

Fig. 1c depicts the loaded waveguide-resonator structure, and the light propagates through the waveguide with leakage into the substrate. The distributions of the transverse-electric (TE) mode for light at $\lambda = 1.55$ μm in the cross section of a suspended PMMA waveguide and placed on silica substrate are shown in Fig. 2a and Fig. 2b, respectively. Note that in the first case the field is mainly concentrated in a mode with $n_{eff} = 1.382$. In the second case, the localized waveguide mode is dissipated and transformed into the delocalized mode with $n_{eff} = 1.415$ in the waveguide/substrate interface. The propagation length of the delocalized mode depends on the mode wavelength, the width and thickness of the waveguide. Fig. 3 presents the dependence of the mode transmission coefficient at $\lambda = 1.55$ μm on the PMMA waveguide thickness and length for the width $w_{nanobeam} = 3$μm. The waveguide is placed on silica substrate with a thickness of 3 μm. We can see that at the waveguide thickness $h_{nanobeam} = 1$ μm the localized mode is transformed into the delocalized one at length more than 50 μm, and more than 90% of light is concentrated in waveguide. In this work, we considered in the first case polymeric PhC nanobeam cavity suspended in air, and in the second case placed one on a silica substrate with a thickness of 3 μm.

The cavity was designed using the deterministic high-Q design method that was introduced in [2]. The key points of the deterministic high-Q design method are a) the zero length of the cavity between the two central holes ($L = 0$) (Fig. 1a), b) the period a of the structure is constant, and c) the Gaussian-like attenuation profile of light, provided by a linear increase of the imaginary part $\gamma = \sigma x$, where σ is the attenuation constant, of the light wave number $k = (1 + i\gamma)\pi/a$ during the propagation of the field along the x-axis of the structure from the central start holes to the end holes of the PhC resonator.

The periodicity of the elliptical holes is constant and $a = 0.612$ μm. To confine an optical field within a specific region of a PhC nanobeam cavity, a defect must be intentionally introduced into the structure. This is typically achieved by gradually altering the periodicity or by modulating the radii of holes or thickness of layers from the center towards the edges. The presence of this defect within the PhC periodic lattice creates a resonant state, manifesting as a transmission peak within the photonic band gap.

On the base of key points of the deterministic design method, we introduce a defect into the structure – a Gaussian tapering mirror, by linearly tapering the elliptical-holes dimensions from the center to both ends. In the taper region, the major axes r_y decreases from 1.313 to 0.578 μm, and the minor axes r_x decreases from 165 to 125 nm. Elliptical holes, compared with circular holes, have larger bandgap and higher reflectivity to confine the optical modes which is important for the low-index contrast PhC nanobeam cavities [1]. Fig. 4a shows the TE dispersion relations – band diagrams of a polymeric 1D PhC nanobeam cavity. We calculate band diagrams for the first structure with periodic elliptical holes with maximum dimensions (blue dashed lines) and for the second structure with minimum dimensions holes (red solid lines) using MEEP. The band for the first structure is higher than the one for the second structure because the band moves to lower frequency when the effective refractive index increases with the holes' dimensions decreasing. The calculated dielectric modes (lower red solid and blue dashed lines) and air modes (upper red solid and blue dashed lines) create photonic band gaps below light line. The cavity resonant frequency ν_{target} = 193.55 THz (λ_{target} = 1.55 μm) is 1% below the edge of the dielectric mode of the central large two holes (lower blue dashed line) with a frequency $\nu_{adjusted}$ = 195.48 THz.

The dependence of the imaginary part γ (mirror strength) of the light wave number $k = (1 + i\gamma)\pi/a$ for different filling fractions $f = \pi r_x r_y / a w_{nanobeam}$, which means the filling fraction of air of the PhC structure unit cell, is showed in Fig. 4b. The mirror strength γ for different filling fractions can be calculated by

$$\gamma = \sqrt{(\omega_2 - \omega_1)^2 / (\omega_2 + \omega_1)^2 - (\omega_{res} - \omega_0)^2 / \omega_0^2}, \quad (1)$$

where ω_2, ω_1, ω_0 are the air band edge, dielectric band edge, and mid-gap frequency of each segment, respectively, ω_{res} is the target cavity resonance [17]. The two central holes with filling factor f_{start} = 0.2896 and radii r_y = 1.313 μm and r_x = 165 nm have γ = 0. The final tapering hole of each side of the PhC resonator with f_{end} = 0.1453 and radii r_y = 0.578 μm and r_x = 125 nm have a maximum value of the mirror strength γ = 0.0183.

The mode volume can be defined as

$$V(\mathbf{r}) = \frac{\int \varepsilon(\mathbf{r}) |\mathbf{E}(\mathbf{r})|^2 d^3\mathbf{r}}{\left[\varepsilon(\mathbf{r}_0) |\mathbf{E}(\mathbf{r}_0)|^2\right]_{max}}, \quad (2)$$

where ε(**r**), **E**(**r**), $\mathbf{r_0}$ are the permittivity, the electric filed strength and the point of interest for observing the enhancement of light-matter interaction, respectively. Figs. 4c and 4d present the dependencies of the polymeric PhC nanobeam cavity Q-factors and mode volumes V on the number of mirror segments N_M of elliptical holes with identical values of radii (r_y = 0.578 μm, r_x = 125 nm) at the ends in the first case of a suspended structure in air, and in the second case placed on silica substate.

In our design, the optimal number of Gaussian tapering mirror segments is N_T = 50 for each side of the PhC cavity. This value of N_T defines the quality of Gaussian-like attenuation profile of the light wave (with $\gamma = \sigma x$). Increasing the numbers of mirror segments N_T and N_M leads to a better light confinement, and, as a consequence, to a higher Q-factor and smaller mode volume V. However, the low index-contrast $n_{cavity}/n_{background}$ = 1.03 of the PMMA PhC nanobeam cavity on a silica substrate leads to scattering losses, light leakage into the substrate, and larger mode volume V.

The transmission spectra of a suspended polymeric PhC nanobeam cavity in air, and placed on a silica substrate are depicted in Fig. 5. Q-factor of a suspended structure at the cavity resonant

wavelength $\lambda = 1.55$ μm is $5 \cdot 10^5$. For the structure placed on a silica substrate $Q = 3 \cdot 10^2$ at $\lambda \sim 1.55$ μm. Note that taking into account the influence of the substrate leads to a shift in the spectrum to the long-wavelength range. Based on the Purcell effect [18], the rate F of spontaneous emission of a quantum emitter in a cavity with resonant frequency λ increases by a factor of

$$F = \frac{3}{4\pi^2}\left(\frac{\lambda}{n_{\text{cavity}}}\right)^3 \frac{Q}{V}. \quad (3)$$

Purcell factor F for suspended PhC nanobeam resonator at $N_M = 50$ is $4.7 \cdot 10^4$, for the structure placed on a silica substrate also at $N_M = 50$ is 26.

CONCLUSIONS

We have presented theoretically and numerically the design of a one-dimensional polymeric PhC nanobeam resonator based on polymethyl-methacrylate and suspended in air, and placed on a silica substrate. Using the three-dimensional finite-difference time-domain method and deterministic high-Q design method, we have demonstrated that a suspended polymeric PhC nanobeam cavity can achieve exceptional optical performance, with a high-Q factor of $Q = 5 \cdot 10^5$, a small mode volume of $V = 0.81(\lambda/n_{\text{cavity}})^3$, and a large Purcell factor of $F = 4.7 \cdot 10^4$ at the telecommunications wavelength of $\lambda = 1.55$ μm. For the structure placed on a silica substrate a maximum Q-factor is $3 \cdot 10^2$, mode volume V is $0.88(\lambda/n_{\text{cavity}})^3$, and Purcell factor F is 26 at $\lambda \sim 1.55$ μm. A suspended architecture for minimizing optical losses and maximizing light confinement in polymer-based systems is important, but challenging in fabrication. For the structure placed on a silica substrate there are possibilities to decrease light scattering and enhance Q/V ratio by changing the width and thickness of the waveguide, and the thickness of a silica substrate. This makes it possible to adjust the dispersion properties of the waveguide, which is interesting for the biphotons generation.

The achieved high Q/V ratio and substantial Purcell factor open a pathway for a new class of flexible and highly efficient photonic devices. The unique combination of the polymer's inherent properties, such as biocompatibility, mechanical flexibility, and ease of fabrication, with high-performance optical confinement suggests many promising applications such as high-sensitively, flexible and implantable biosensors, low-threshold tunable lasers, small efficient LEDs, on-chip quantum information processing.

FUNDING

Theoretical research and computational work of the photonic crystal nanobeam resonator were supported by the Ministry of Science and Higher Education of the Russian Federation (R&D Reg. 125012300688-6). The calculations of waveguides properties were sponsored by the program of strategic academic leadership of KNRTU-KAI named after A. N. Tupolev (“PRIORITY 2030”), R&D Reg. 125070808154-3.

CONFLICT OF INTEREST

The authors declare that they have no conflicts of interest.

REFERENCES

1. Quan, Q., Burgess, I.B., Tang, S.K.Y., Floyd, D.L., Loncar, M. High-Q, low index-contrast polymeric photonic crystal nanobeam cavities, *Optics Express*, 2011, vol. 19, no. 22, p. 22191. https://doi.org/10.1364/oe.19.022191

2. Quan, Q., Loncar, M. Deterministic design of wavelength scale, ultra-high Q photonic crystal nanobeam cavities, *Optics Express*, 2011, vol. 19, no. 19, p. 18529. https://doi.org/10.1364/OE.19.018529

3. Gainutdinov, R.Kh., Garifullin, A.I., Khamadeev, M.A. Effect of Changing the Electron Mass and Physicochemical Processes in One-Dimensional Photonic Crystals, *Bulletin of the Lebedev Physics Institute*, 2019, vol. 46, no. 4, p. 115. https://doi.org/10.3103/S106833561904002X

4. Yang, D.-Q., Duan, B., Liu, X., Wang, A.-Q., Li, X.-G., Ji, Y.-F. Photonic Crystal Nanobeam Cavities for Nanoscale Optical Sensing: A Review, *Micromachines*, 2020, vol. 11, no. 72, p. 1. https://doi:10.3390/mi11010072

5. Garifullin, A.I., Gainutdinov, R.Kh., Khamadeev, M.A. Controlling the frequencies of photons emitted by a single quantum dot in a one-dimensional photonic crystal, *Journal of Optical Technology*, 2024, vol. 91, no. 6, p. 399. https://doi.org/10.1364/JOT.91.000399

6. Bykov, V.P. Spontaneous Emission in a Periodic Structure, *Soviet Journal of Experimental and Theoretical Physics*, 1972, vol. 35, no. 2, p. 269.

7. Yablonovitch, E. Inhibited spontaneous emission in solid-state physics and electronics, *Physical Review Letters*, 1987, vol. 58, no. 20, p. 2059. https://doi.org/10.1103/PhysRevLett.58.2059

8. Gainutdinov, R.Kh., Garifullin, A.I., Khamadeev, M.A., Salakhov, M.Kh. Quantum electrodynamics in photonic crystals and controllability of ionization energy of atoms, *Physics Letters A*, 2021, vol. 404, no. 127407, p. 1. https://doi.org/10.1016/j.physleta.2021.127407

9. Gainutdinov, R.Kh., Nabieva, L.Ya., Garifullin, A.I., Shirdelkhavar, A., Mutygullina, A.A., Salakhov, M.Kh. Strong interaction effects in the emission spectra of a quantum dot coupled to a phonon reservoir, *JETP Letters*, 2021, vol. 114, no. 4, p. 188. https://doi.org/10.1134/S0021364021160050

10. Garifullin, A.I., Gainutdinov, R.Kh., Khamadeev, M.A. Acceleration of Chemical Reactions in Hybrid One-Dimensional Photonic Crystals Based on High-Index Metamaterials, *Bulletin of the Russian Academy of Sciences: Physics*, 2022, vol. 86**,** no. 1, p. S66. https://doi.org/10.3103/S106287382270040X

11. Garifullin, A.I., Arslanov, N.M. Optimization of SI_3N_4 nanophotonic resonator taking into account the substrate influence, *Proceedings of SPIE*, 2024, vol. 13168, p. 1. https://doi.org/10.1117/12.3026578

12. Garifullin, A.I., Arslanov, N.M. Determination of Spectral and Mode Properties of Nanophotonic Cavities Based on Silicon and Silicon Nitride, *Bulletin of the Russian Academy of Sciences: Physics*, 2025, vol. 89, no. 12, p. 2278. https://doi.org/10.1134/S1062873825713534

13. Clevenson, H., Desjardins, P., Gan, X., Englund, D. High sensitivity gas sensor based on high-Q suspended polymer photonic crystal nanocavity, *Applied Physics Letters*, 2014, vol. 104, no. 241108, p. 1. https://doi.org/10.1063/1.4879735

14. Gan, X., Clevenson, H., Englund, D. Polymer photonic crystal nanocavity for precision strain sensing, *ACS Photonics*, 2017, vol. 4, no. 7, p. 1591. https://doi.org/10.1021/acsphotonics.7b00030

15. Li, X., Liu, X., Qin, Y., Yang, D., Ji, Y. Ultra-low index-contrast polymeric photonic crystal nanobeam electro-optic modulator, *IEEE Photonics Journal*, 2020, vol. 12, no. 3, p. 1. https://doi.org/10.1109/JPHOT.2020.2994241
16. Deotare, P.B., McCutcheon, M.W., Frank, I.W., Khan, M., Loncar, M. High quality factor photonic crystal nanobeam cavities, *Applied Physics Letters*, 2009, vol. 94, no. 121106, p. 12. https://doi.org/10.1063/1.3107263
17. Quan, Q., Deotare, P.B., Loncar, M. Photonic crystal nanobeam cavity strongly coupled to the feeding waveguide, *Applied Physics Letters*, 2010, vol. 96, no. 203102, p. 1. https://doi.org/10.1063/1.3429125
18. Purcell, E.M. Spontaneous Emission Probabilities at Radio Frequencies, *Physical Review*, 1946, vol. 69, p. 681. https://doi.org/10.1007/978-1-4615-1963-8_40

FIGURE CAPTIONS

Fig. 1. (a) Schematic representation of a 1D PhC nanobeam cavity consisting of a PMMA waveguide with the width w_{nanobeam} = 3 μm and the thickness h_{nanobeam} = 1 μm, and a periodic array of elliptical holes with a period a = 0.612 μm. Gaussian tapering mirror segments have N_{T} holes, and mirror segments have N_{M} holes with the constant dimensions. The structure is symmetric with respect to the central black dashed line. The structure is considered as (b) suspended in air and as (c) placed on a SiO_2/Si substrate.

Fig. 2. The distributions of the TE-mode for light at λ = 1.55 μm in the cross section of (a) a suspended PMMA waveguide and (b) placed on silica substrate correspond to the structures in Fig. 1b and Fig. 1c, respectively. The width of the polymeric waveguide is w_{nanobeam} = 3μm, the thickness is h_{nanobeam} = 1 μm.

Fig. 3. The dependence of the TE-mode transmission coefficient at λ = 1.55 μm on the PMMA waveguide thickness and length for the width w_{nanobeam} = 3μm. The waveguide is placed on silica substrate with a thickness of 3 μm.

Fig. 4. (a) TE-polarization band diagram for a 1D PhC nanobeam cavity with elliptical holes, in the first case, with filling factor f_{start} = 0.2896 (blue dashed line) and, in the second case, with f_{end} = 0.1453 (red solid line). $g = 2\pi/a$ is the reciprocal lattice constant of the structure. The green dotted line indicates a light line in a vacuum ($\omega = ck_x$). The cavity resonant frequency ν_{target} = 193.55 THz is 1% below the edge of the dielectric mode (lower blue dashed line) with a frequency ν_{adjusted} = 195.48 THz. (b) The dependence of the imaginary part γ (mirror strength) of the light wave number $k = (1 + i\gamma)\pi/a$ for different filling fractions. The two central elliptical holes with f_{start} = 0.2896 and radii r_y = 1.313 μm and r_x = 165 nm have γ = 0. The final tapering hole of each side of the PhC resonator with f_{end} = 0.1453 and radii r_y = 0.578 μm and r_x = 125 nm have a maximum value of the mirror strength γ = 0.0183. (c) Q-factors (log(10) scale) in the first case of a suspended PhC nanobeam cavity in air, and in the second case placed on a silica substrate, for different number of mirror segments N_{M} of holes with r_y = 0.578 μm and r_x = 125 nm added on both ends of the structure. (d) Mode volumes ($V/(\lambda/n_{\text{cavity}})^3$) at λ = 1.55 μm in the first case of a suspended PhC nanobeam cavity in air, and in the second case placed on a silica substrate, for different number of mirror segments N_{M} of holes with r_y = 0.578 μm and r_x = 125 nm added on both ends of the structure.

Fig. 5. The transmission spectra of a suspended polymeric PhC nanobeam cavity in air, and placed on a silica substrate with N_{T} =50, N_{M} = 50. In the first case Q-factor is $5 \cdot 10^5$ at the cavity resonant telecommunications wavelength λ = 1.55 μm, in the second case $Q = 3 \cdot 10^2$ at λ ~ 1.55 μm.

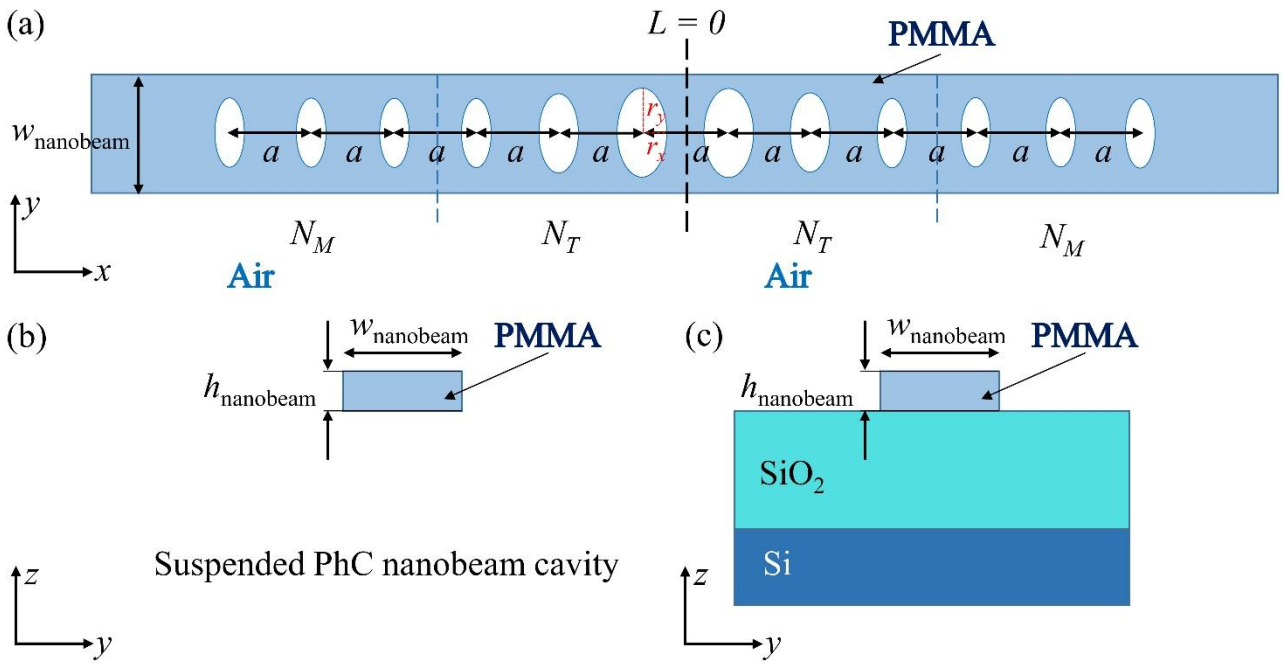
(a)
L = 0
PMMA
w nanobeam
a
r y
r x
y
x
N M
N T
N T
N M
Air
Air
(b)
w nanobeam
PMMA
h nanobeam
Suspended PhC nanobeam cavity
z
y
(c)
w nanobeam
PMMA
h nanobeam
SiO2
Si
z
y

Fig. 1.

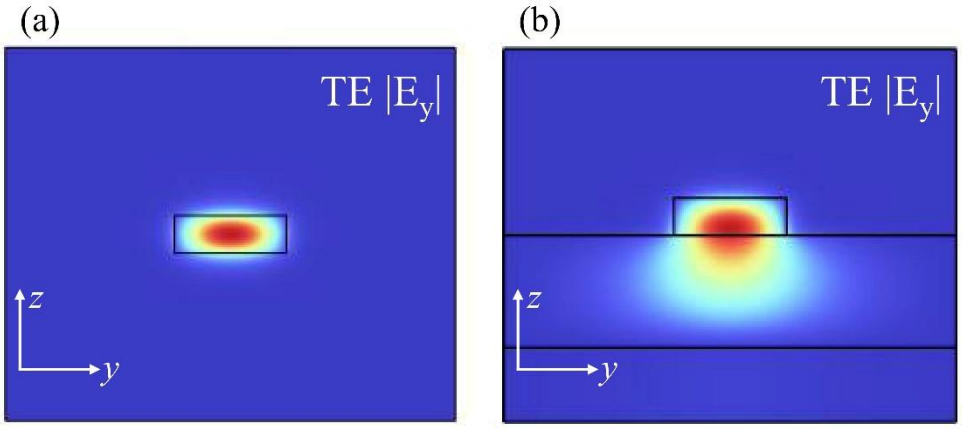
(a)
TE |Ey|
z
y
(b)
TE |Ey|
z
y

Fig. 2.

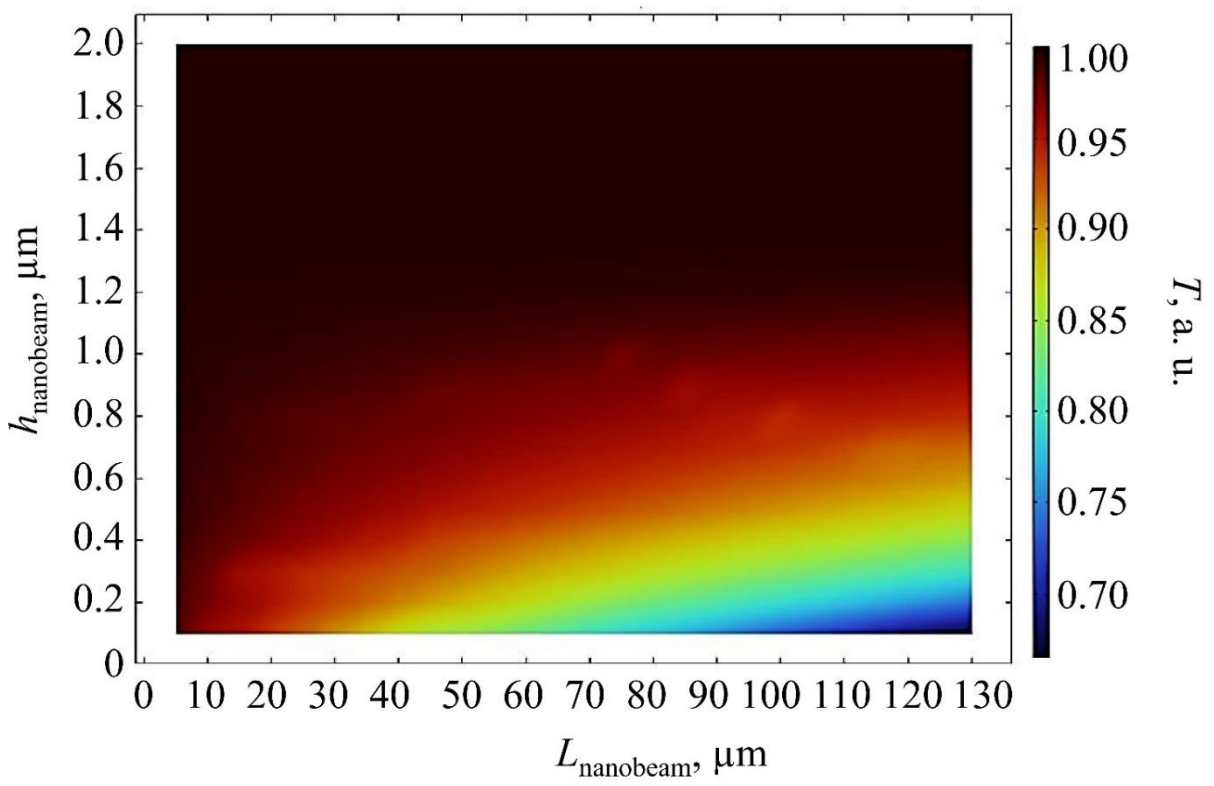
2.0
1.8
1.6
1.4
1.2
1.0
0.8
0.6
0.4
0.2
0
h_{nanobeam}, μm
0 10 20 30 40 50 60 70 80 90 100 110 120 130
L_{nanobeam}, μm
1.00
0.95
0.90
0.85
0.80
0.75
0.70
T, a. u.

Fig. 3.

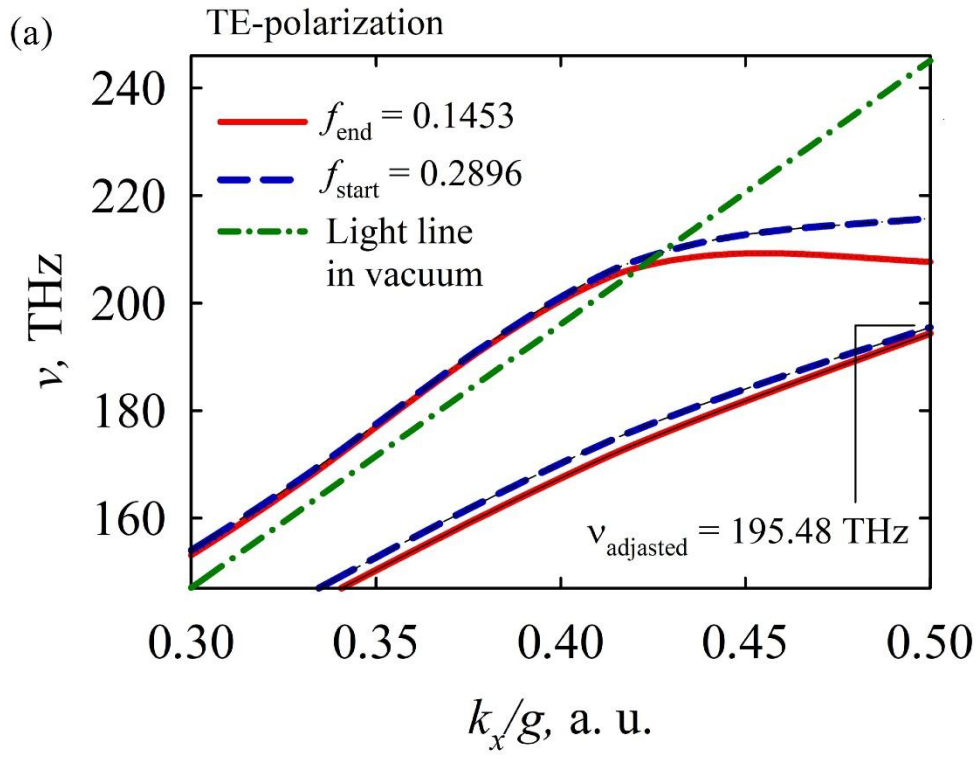
(a)
TE-polarization
240
220
200
180
160
ν, THz
f_{end} = 0.1453
f_{start} = 0.2896
Light line
in vacuum
$\nu_{adjasted}$ = 195.48 THz
0.30
0.35
0.40
0.45
0.50
k_x/g, a. u.

Fig. 4a.

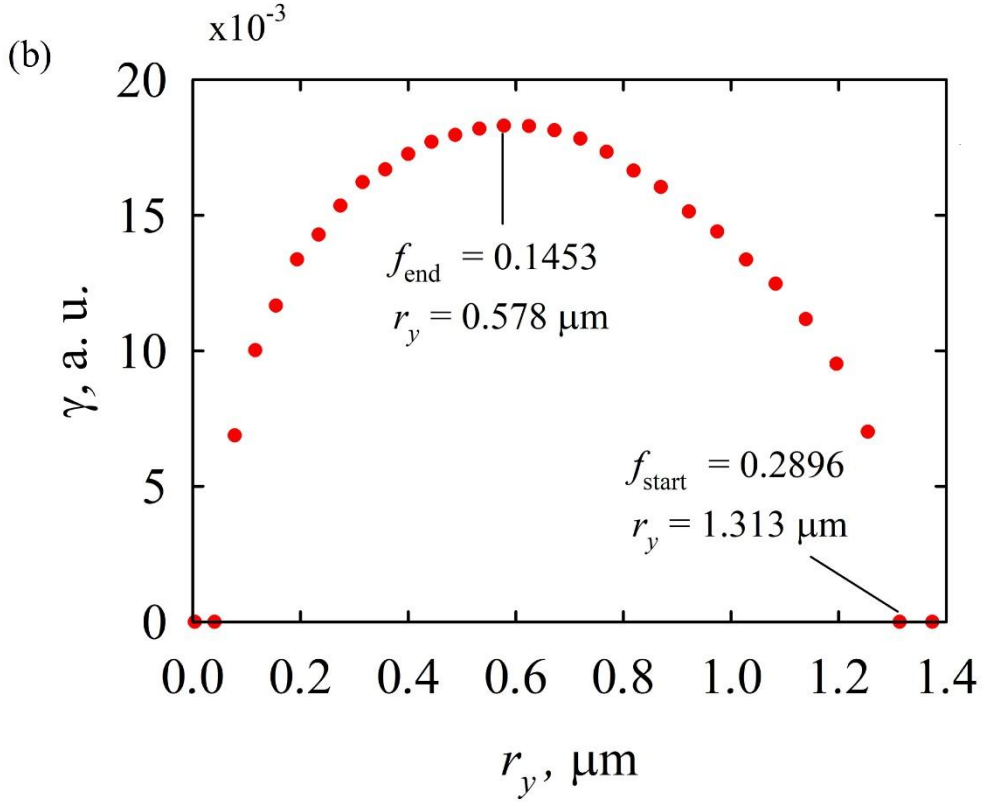
(b)
x10^{-3}
20
15
10
5
0
γ, a. u.
f_{end} = 0.1453
r_y = 0.578 μm
f_{start} = 0.2896
r_y = 1.313 μm
0.0
0.2
0.4
0.6
0.8
1.0
1.2
1.4
r_y, μm

Fig. 4b.

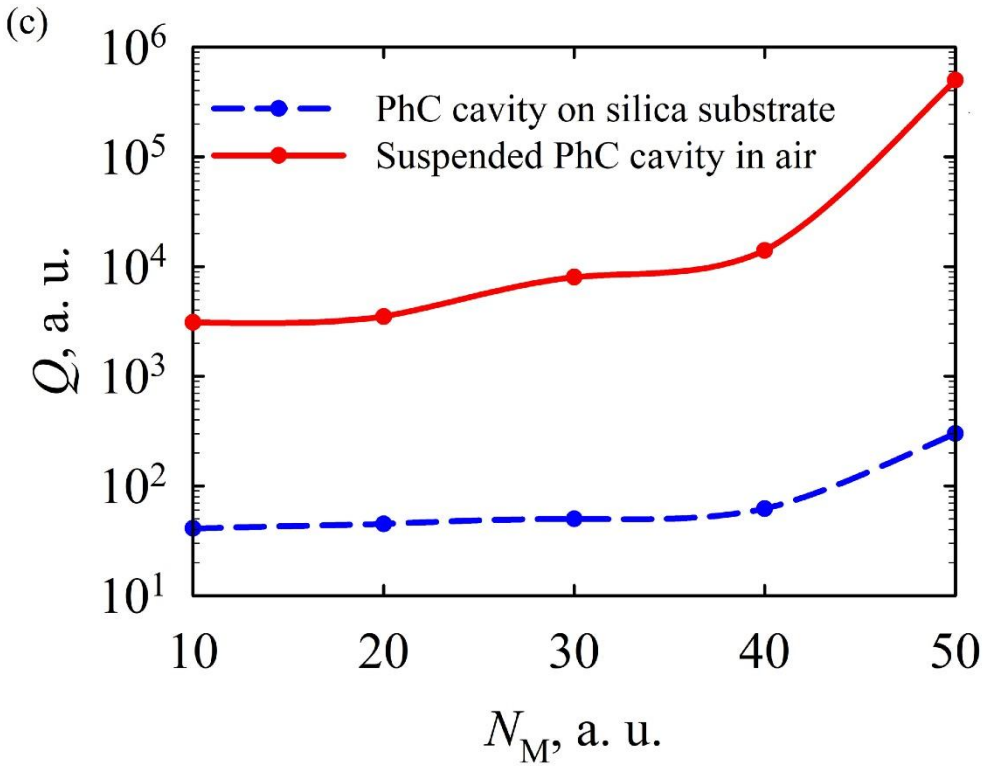
(c)
10^6
10^5
10^4
10^3
10^2
10^1
Q, a. u.
PhC cavity on silica substrate
Suspended PhC cavity in air
10
20
30
40
50
N_M, a. u.

Fig. 4c.

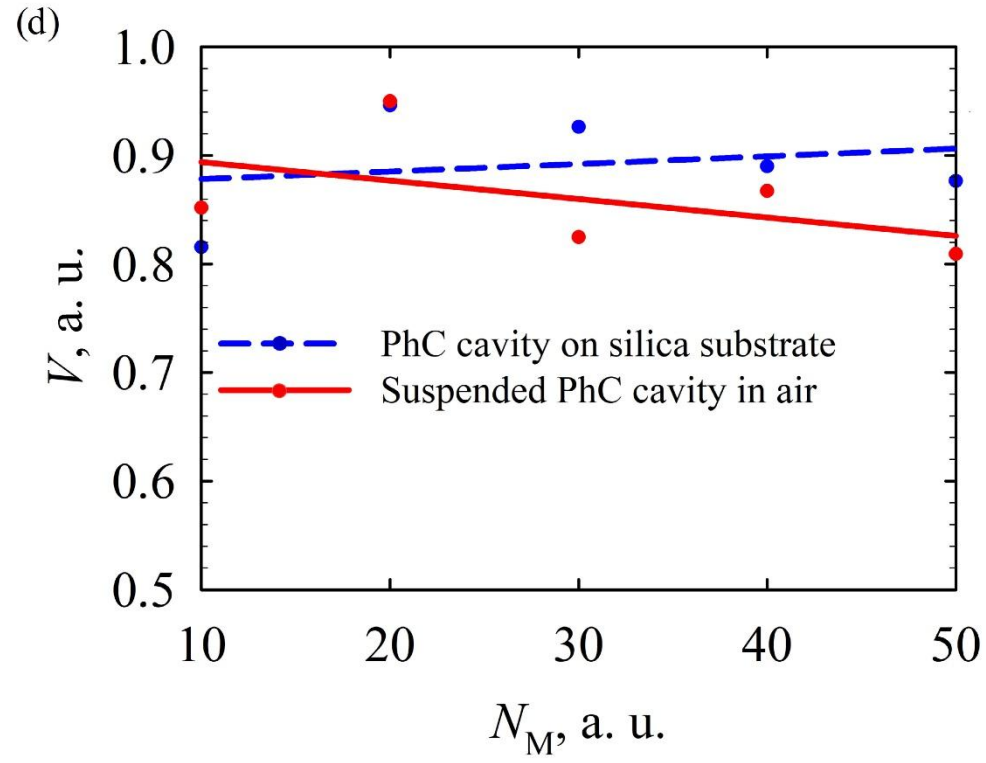
(d)
1.0
0.9
0.8
0.7
0.6
0.5
V, a. u.
PhC cavity on silica substrate
Suspended PhC cavity in air
10
20
30
40
50
N_M, a. u.

Fig. 4d.

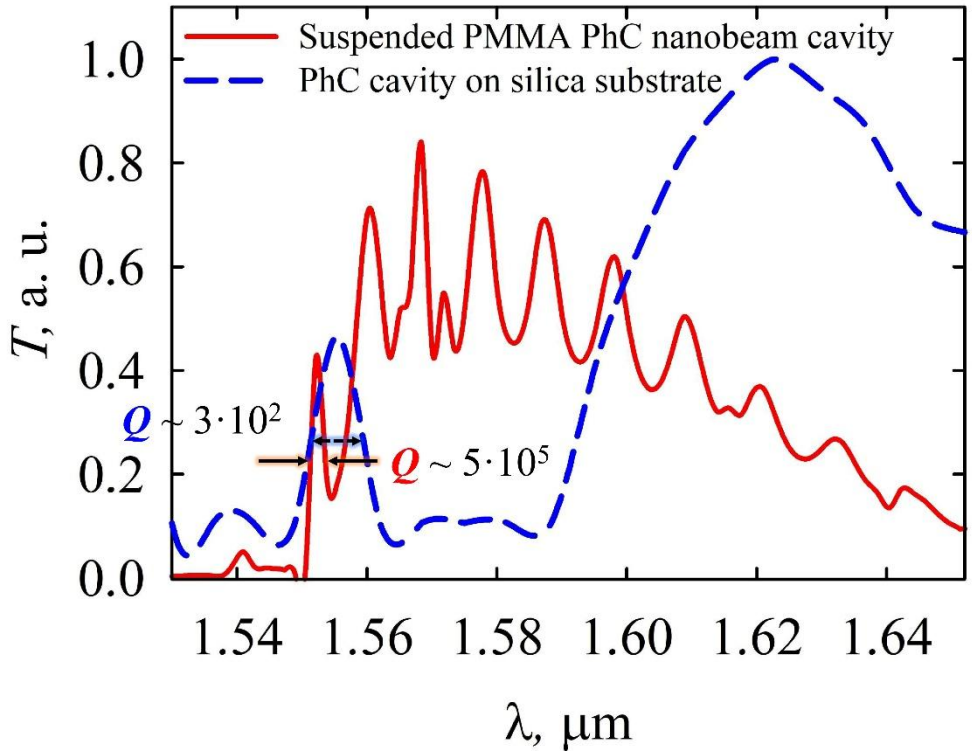
Suspended PMMA PhC nanobeam cavity
PhC cavity on silica substrate
T, a. u.
1.0
0.8
0.6
0.4
0.2
0.0
Q ~ 3·10²
Q ~ 5·10⁵
1.54
1.56
1.58
1.60
1.62
1.64
λ, μm

Fig. 5.